KI REPORTS
KIReports.org
TRANSLATIONAL RESEARCH

Urine Single-Cell RNA Sequencing in Focal Segmental Glomerulosclerosis Reveals Inflammatory Signatures

Khun Zaw Latt[1,16], Jurgen Heymann[1,16], Joseph H. Jessee[1], Avi Z. Rosenberg[2], Celine C. Berthier[3], Arnon Arazi[4], Sean Eddy[3], Teruhiko Yoshida[1], Yongmei Zhao[5], Vicky Chen[5], George W. Nelson[5], Margaret Cam[5], Parimal Kumar[6], Monika Mehta[6], Michael C. Kelly[7], Matthias Kretzler[3], The Nephrotic Syndrome Study Network (NEPTUNE), The Accelerating Medicines Partnership in Rheumatoid Arthritis and Systemic Lupus Erythematosus (AMP RA/SLE) Consortium; Patricio E. Ray[8], Marva Moxey-Mims[9,10], Gregory H. Gorman[11,12], Brent L. Lechner[11,12], Renu Regunathan-Shenk[13], Dominic S. Raj[13], Katalin Susztak[14], Cheryl A. Winkler[15] and Jeffrey B. Kopp[1]

[1]Kidney Disease Section, Kidney Diseases Branch, National Institute of Diabetes and Digestive and Kidney Diseases, National Institutes of Health, Bethesda, Maryland, USA; [2]Department of Pathology, Johns Hopkins Medical Institutions, Baltimore, Maryland, USA; [3]Division of Nephrology, Department of Internal Medicine, Michigan Medicine, Ann Arbor, Michigan, USA; [4]The Feinstein Institute for Medical Research, Northwell Health, Manhasset, New York, USA; [5]Advanced Biomedical and Computational Sciences, Frederick National Laboratory for Cancer Research, Leidos Biomedical Research, Inc., National Cancer Institute, Frederick, Maryland, USA; [6]Center for Cancer Research Sequencing Facility, Cancer Research Technology Program, Frederick National Laboratory for Cancer Research, Leidos Biomedical Research, Inc., Frederick, Maryland, USA; [7]Cancer Research Technology Program, Single-Cell Analysis Facility, Frederick National Laboratory for Cancer Research, National Cancer Institute, Frederick, Maryland, USA; [8]Department of Pediatrics, Child Health Research Center, University of Virginia, Charlottesville, Virginia, USA; [9]Division of Nephrology, Children's National Hospital, Washington, District of Columbia, USA; [10]Department of Pediatrics, The George Washington University School of Medicine and Health Sciences, Washington, District of Columbia, USA; [11]Section on Pediatric Nephrology, Walter Reed National Military Medical Center, Bethesda, Maryland, USA; [12]Department of Pediatrics, Uniformed Services University, Bethesda, Maryland, USA; [13]Division of Kidney Disease and Hypertension, The George Washington University School of Medicine and Health Sciences, Washington DC, USA; [14]Department of Medicine, Renal Electrolyte and Hypertension Division, Department of Genetics, Perelman School of Medicine, University of Pennsylvania, Philadelphia, Pennsylvania, USA; and [15]Basic Research Program, Frederick National Laboratory for Cancer Research, Frederick, Maryland, USA

Introduction: Individuals with focal segmental glomerular sclerosis (FSGS) typically undergo kidney biopsy only once, which limits the ability to characterize kidney cell gene expression over time.

Methods: We used single-cell RNA sequencing (scRNA-seq) to explore disease-related molecular signatures in urine cells from subjects with FSGS. We collected 17 urine samples from 12 FSGS subjects and captured these as 23 urine cell samples. The inflammatory signatures from renal epithelial and immune cells were evaluated in bulk gene expression data sets of FSGS and minimal change disease (MCD) (The Nephrotic Syndrome Study Network [NEPTUNE] study) and an immune single-cell data set from lupus nephritis (Accelerating Medicines Partnership).

Results: We identified immune cells, predominantly monocytes, and renal epithelial cells in the urine. Further analysis revealed 2 monocyte subtypes consistent with M1 and M2 monocytes. Shed podocytes in the urine had high expression of marker genes for epithelial-to-mesenchymal transition (EMT). We selected the 16 most highly expressed genes from urine immune cells and 10 most highly expressed EMT genes from urine podocytes as immune signatures and EMT signatures, respectively. Using kidney biopsy transcriptomic data from NEPTUNE, we found that urine cell immune signature and EMT signature genes were more highly expressed in FSGS biopsies compared with MCD biopsies.

Correspondence: Khun Zaw Latt, Kidney Disease Section, Kidney Diseases Branch, National Institute of Diabetes and Digestive and Kidney Diseases, National Institutes of Health, 10 Center Drive, 3N114, Bethesda, Maryland 20892-1268, USA. E-mail: khunzaw.latt@nih.gov

[16]KZL and JH contributed equally to this work.

The complete list of The Nephrotic Syndrome Study Network (NEPTUNE) enrolling centers appears in the Supplementary Note S1.

Received 10 September 2021; revised 29 October 2021; accepted 1 November 2021; published online 25 November 2021

Conclusion: The identification of monocyte subsets and podocyte expression signatures in the urine samples of subjects with FSGS suggests that urine cell profiling might serve as a diagnostic and prognostic tool in nephrotic syndrome. Furthermore, this approach may aid in the development of novel biomarkers and identifying personalized therapies targeting particular molecular pathways in immune cells and podocytes.

Kidney Int Rep (2022) **7,** 289–304; https://doi.org/10.1016/j.ekir.2021.11.005
KEYWORDS: FSGS; inflammation and fibrosis; profibrotic signatures; single cell RNA-seq; urine biomarkers

See Commentary on Page 138

FSGS and MCD are the major causes of primary nephrotic syndrome and manifest similar clinical features. Establishing the correct diagnosis of these diseases is important to initiate effective treatments. Patients with MCD usually respond well to glucocorticoid therapy and usually have excellent long-term prognosis. In contrast, patients with FSGS are often resistant to glucocorticoid therapy and have progressive decline in glomerular filtration rate.[1,2] Currently, kidney biopsy is the principal method for the histologic diagnosis of nephrotic diseases. Nevertheless, biopsy is an invasive procedure that is sometimes deferred, particularly in children, and is typically performed only once in adults. Owing to sampling limitations and the focal distribution of lesions in FSGS, biopsy can also fail to distinguish MCD from early FSGS. Moreover, the current approaches to renal biopsy analysis provide limited information on molecular mechanisms of complex diseases, such as FSGS.

In recent years, scRNA-seq has emerged as a powerful tool to characterize single-cell transcriptomes from various sources. Several reviews of this methodology, as applied to kidney research, have been published recently.[3–6] These studies have applied single-cell or nuclear RNA-seq approaches to kidney tissue. We hypothesized that urine from patients with kidney diseases could be a useful, noninvasive source of information on the disease and that urine scRNA-seq could add valuable transcriptional information on injured primary renal parenchymal cells that appear in the urine, including podocytes and tubular epithelial cells and reactive cells, such as immune cells, and could distinguish these cells from urothelial cells. This transcriptional information might inform clinicians on mechanisms of injury and suggest targeted therapies. To evaluate the urine cells for potential application as a diagnostic tool for FSGS and to uncover the molecular mechanisms of the disease at the single-cell level, we performed scRNA-seq of urine samples from subjects with FSGS.

METHODS

Study Design

We collected a total of 17 non–first-void morning urine samples from 12 subjects and captured these as 23 cell samples using Chromium Single Cell 3′ Library & Gel Bead Kit, version 2 (10x Genomics, Pleasanton, CA). Details of the clinical features of subjects and sample preparation can be found in Table 1, Supplementary Figure S12 and Supplementary Methods.

Urine Sample Processing and Single-Cell Capture

Subjects were asked to collect second daily urine using clean-catch practices 2 to 4 hours after the first morning void. Whole urine samples (50–100 ml) were filtered (70 μm) and then sedimented for 10 to 15 minutes at 300 × *g* at 4 °C. The sediment (cell pellet) was washed twice with ice-cold 0.04% bovine serum albumin in Dulbecco's phosphate-buffered saline and then subjected either to fluorescence-activated cell sorting (8 cell samples) or to immediate cell capture using the 10x Genomics platform (15 cell samples) (Supplementary Figure S13 and Supplementary Table S16).

For fluorescence-activated cell sorting, urine cells were buffer-exchanged into Flow Cytometry Staining Buffer (eBioscience, Invitrogen, Carlsbad, CA), passed through a 40-μm filter, and combined with 7-aminoactinomycin D and fluorescence marker and HOECHST DNA stain. Debris-free, nucleated live cells were selected using a BDFASC Fusion device (BD Biosciences, San Jose, CA) with a 70 μm nozzle size at 70 psi sheath pressure. HOECHST-positive, 7-aminoactinomycin D-positive cells were sorted into Dulbecco's phosphate-buffered saline (Thermofisher, Waltham, MA) with 10% fetal bovine serum (Neuromics, Edina, MN) and then subjected to immediate cell capture.

Urine cells were captured for scRNA-seq using Chromium Single Cell 3′ Library & Gel Bead Kit, version 2. Captured cells were processed following exactly the supplier's protocol. The resulting mRNA libraries were sequenced on NextSeq 500 platform (Illumina, San Diego, CA) with typical setup as a 26 cycles + 57 cycles nonsymmetric run. Demultiplexing was done, allowing 1 mismatch per barcode. Sequencing data were analyzed with the Cell Ranger version 2.2.0 software (10x Genomics) applying default parameters. Results from the analysis are found in

Table 1. Demographic characteristics of study participants

Study participants	No. of urine samples	No. of cell samples	Age	Sex	Ethnicity	UPCR (at urine collection)	UPCR (highest recorded)	eGFR	Glucocorticoid responsiveness	APOL1 status	Summary of biopsy findings
Subject 1[a]	5	7	37	Male	African American	4.56 (4.23–5.04)	7.74	86 (79–86)	Resistant	G1G2	FSGS, diffuse foot process effacement, interstitial fibrosis, and tubular atrophy 15%–17%
Subject 2[a]	2	4	45	Female	African American	4.99 (4.08–5.9)	7.3	38 (38–38)	Partial remission	Not available	FSGS, interstitial fibrosis, and tubular atrophy 30%, moderate arteriosclerosis
Subject 3	1	2	69	Female	African American	0.22	10.3	28	Resistant	G1G0	Arterio-nephrosclerosis
Subject 4[a]	1	2	37	Male	Asian American	2.83	2.83	45	Not used	G0G0	FSGS, 60% segmentally sclerosed glomeruli, moderate interstitial fibrosis and mild to moderate vascular sclerosis
Subject 5[a]	1	1	60	Female	European American	4.84	19.6	25	Resistant	G0G0	FSGS, podocyte enlargement and extensive effacement of foot processes, extensive interstitial fibrosis, and tubular atrophy
Subject 6	1	1	48	Female	European American	0.39	1.6	85	Not used	Not available	FSGS (early), minimal tubular atrophy and interstitial fibrosis
Subject 7	1	1	26	Male	Middle Eastern	0.17	0.303	54	Not used	Not available	Single functioning kidney with no biopsy
Subject 8	1	1	13	Male	African American	3.47	3.47	119	Partial remission	Not available	MCD
Subject 9	1	1	18	Male	African American	Undetectable	Undetectable	79	Not used	Not available	FSGS, 7 of 23 glomeruli had global sclerosis, remaining glomeruli without focal sclerosis or increased cellularity
Subject 10[a]	1	1	75	Male	European American	11.06	11.06	17	Resistant	G0G0	FSGS, perihilar type, moderate arteriosclerosis with mild tubulointerstitial scarring, early diabetic glomerulopathy
Subject 11[a]	1	1	63	Female	African American	0.77	3.0	30	Resistant	G0G0	FSGS, segmental increase in mesangial matrix, moderate tubular atrophy and interstitial fibrosis, patchy dense inflammatory infiltrate
Subject 12[a]	1	1	51	Male	European American	0.62	3.6	18	Not used	Not available	FSGS with some global sclerosis, diffuse tubular atrophy and interstitial fibrosis, focal acute tubular atrophy, arteriosclerosis and arteriolar hyalinosis

eGFR, estimated glomerular filtration rate; FSGS, focal segmental glomerular sclerosis; MCD, minimal change disease; UPCR, urine protein to creatinine ratio.
[a]Denotes the 7 biopsy-proven subjects with FSGS with urine protein-to-creatinine ratio > 0.5. The 7-sample analysis included 1 sample from each of these 7 subjects. The details of 3 subjects without biopsy evidence of FSGS (subjects 3, 7M and 8) are presented in the Supplementary Methods section. The urine protein-to-creatinine ratio and eGFR values for subjects 1 and 2 are the median and the interquartile range calculated from 5 and 2 measurements, respectively.

Supplementary Figure S14 and Supplementary Table S16.

Data Integration and Batch Correction

Single-cell gene expression data from all 23 cell samples were merged into a single data set using Seurat (version 2.3.4, https://satijalab.org/seurat/).[7] Cells with fewer than 100 detected genes or more than 6000 detected genes and cells with mitochondrial transcripts representing >10% of all transcripts were removed. After filtering, there were 5551 cells remained for downstream analysis. Data were batch-corrected by the sample identities using the Harmony R package (version 0.1.0).[8] Pseudotime analysis of monocytes was done by using Monocle2 R package,[9] and cell-cell interaction analysis was done by CellPhoneDB.[10,11] Additional details of scRNA-seq and bulk transcriptomic analysis can be found in the Supplementary Methods.

Data Availability

The single-cell RNA-seq raw data have been deposited in the National Center for Biotechnology Information Gene Expression Omnibus database and are accessible through Gene Expression Omnibus accession number, GSE176465 at https://www.ncbi.nlm.nih.gov/geo/query/acc.cgi?acc=GSE176465.

RESULTS

Study Design for Single-Cell RNA Seq of FSGS Urine Cells

To analyze gene expression signatures of single cells in the urine, we performed scRNA-seq of 23 cell samples, derived from 17 urine samples obtained from 12 subjects with FSGS (Table 1). Using known canonical marker genes, we identified clusters that are most likely podocytes, tubular epithelial cells, and immune cells (monocytes and lymphocytes). We evaluated expression levels of immune cell-specific genes in glomerular and tubulointerstitial expression data from the NEPTUNE cohort. We were able to distinguish subjects with FSGS and those with MCD based on the expression of these genes in the NEPTUNE data set.

Most of the immune cells in the urine samples were monocytes. We compared urine monocytes with monocyte data from a healthy peripheral blood mononuclear cell (PBMC) data set from 10x Genomics and identified M1 and M2 monocyte subtypes with distinct gene expression profiles. We also used *in silico* approaches to annotate M1 and M2 subtypes and to reveal that their gene expression signatures were similar to those in another inflammatory kidney disease, lupus nephritis, using single-cell immune data from lupus nephritis biopsy samples from the Accelerating Medicines Partnership SLE consortium. Finally, we performed cell-cell interaction analysis and identified interactions of tumor necrosis factor (TNF) family cytokines between immune and renal epithelial cells, which could be potential targets for immunotherapy.

Identification of Different Cell Types in the Urine of Patients With FSGS

Unsupervised clustering identified 15 cell clusters (Figure 1a), with cells from multiple samples present in most clusters (Figure 1b and Supplementary Figure S1 and Supplementary Table S1). We confirmed that there were no substantial batch effects at the gene expression level among the samples (Supplementary Note S2 and Supplementary Figures S5 and S6). We used known canonical marker genes for kidney and immune cells to identify the cell type of each cluster (Supplementary Figure S2).

We identified a podocyte cluster that expressed the podocyte marker genes *WT1*, *PLA2R1*, and *SYNPO* (Supplementary Figure S2C) and parietal epithelial cell (PEC) markers, such as *PAX2*, *PAX8*, and *CLDN1* (Supplementary Figure S3). Other canonical podocyte marker genes, such as *PODXL* and *NPHS1*, were not strongly expressed in the urinary podocytes, which may reflect an altered transcriptional state of podocytes as a consequence of being shed into the urine. For the podocyte cluster, the most highly expressed gene, compared with all the remaining clusters, was *IGFBP7*, a marker that has also been reported for podocytes.[12] Among other top expressed genes were myofibroblast markers (*CTGF*, *MYL9*), mesenchymal markers (*VIM*, *THY1*), extracellular matrix proteins (*MMP7*, *CAV1*), markers for smooth muscle differentiation (*CALD1*, *TPM1*, and *TAGLN*), and *CRYAB*, which induces epithelial-to-mesenchymal transition (EMT) (Supplementary Table S2).[13]

Tubular cell cluster expressed *POU3F3*, *UMOD*, and *FXYD2*. This cluster also had high expression of *TPM1* and *CRYAB*, consistent with EMT. There were also a small collecting ductal cell cluster, identified by high expression of *AQP2*, and a myofibroblast cluster, identified by high expression of *TAGLN*, *MYL9*, and *ACTA2*. The remaining clusters were 7 epithelial cell clusters expressing *KRT6A*, *KRT13*, *KRT15*, and *KRT17*, and likely originated from different segments of the male and female genitourinary tracts (Supplementary Figure S2).

We identified 3 monocyte clusters (MCs) (MC1, MC2, and MC3), comprising a total of 1040 cells, which expressed *CD14* and *FCGR3A* (CD16). The 3 MCs shared some highly expressed genes, including *FCER1G*, *TYROBP*, and *HLA* genes. The most highly expressed genes for MC1 included *TIMP1*, *CCL2*, and *IL1B*, and those for MC2 included *APOE*, *C1QB*, and

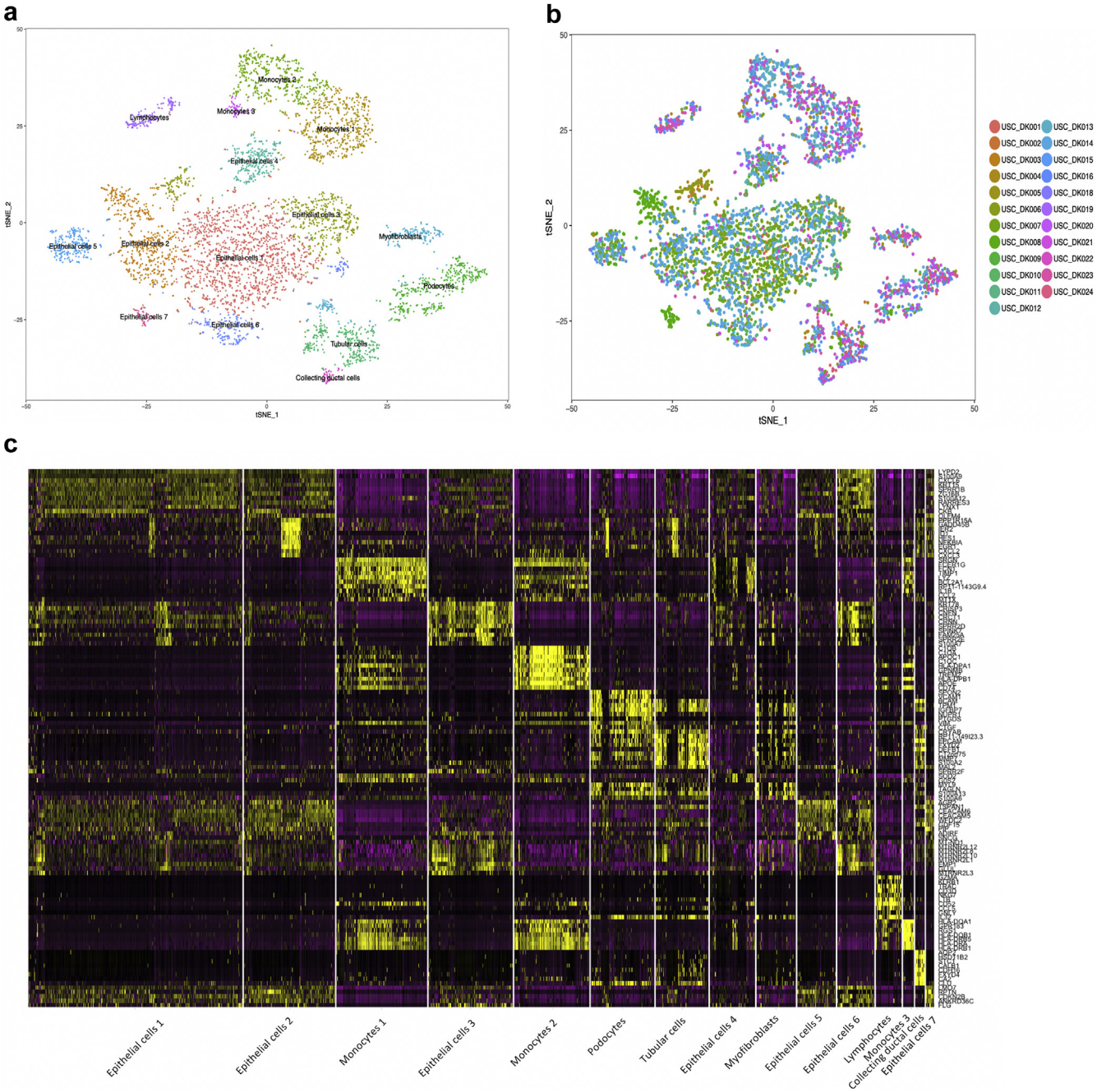

Figure 1. Urine cell type clusters and gene expression profiles. (a) Batch-corrected t-SNE plot of urine single-cell aggregate data from all 23 cell samples derived from 17 urine samples revealing 15 individual cell clusters and cell types. (b) The same t-SNE plot with a different color for each sample. (c) Principal component heatmap plot revealing 10 most highly expressed genes in each of 15 clusters (vertical columns), with each row representing 1 gene, with high expression (yellow), intermediate expression (purple), and low expression (black). t-SNE, t-distributed stochastic neighbor embedding.

APOC1. MC3 had strong expression of *HLA* class II genes and *CD74* (Figure 1c), suggesting the differentiation toward dendritic cells and manifesting active antigen presentation to T cells.[14] This cluster also had the highest expression of dendritic cell marker genes, such as *CD1C*, *CD1E*, *CCR7*, *FCER1A*, and *CLEC10A* (Supplementary Figure S4).

We observed a single lymphocyte cluster expressing *CD3G* and *GZMA*. The lymphocyte cluster was mostly composed of T lymphocytes with high expression of cytotoxic genes, including *GNLY*, *GZMA*, and *LTB*, and a smaller subgroup of B cells expressing *CD19* and *MS4A1* (Figure 1c and Supplementary Figures S2A and S2E). Because there were several samples from some subjects, we confirmed these results by repeating the analysis using 1 sample from each of biopsy-proven subjects with FSGS (Supplementary Note S3 and Supplementary Tables S8–S10).

Table 2. The most up-regulated genes in FSGS monocytes from all 23 cell samples ($n = 1040$ cells) compared with healthy peripheral blood monocytes from 1 healthy subject ($n = 1906$ cells)

Top FSGS monocyte genes	avg_logFC	Fraction.1 (urine)	Fraction.2 (PBMC)	P_val_adj
APOE	4.14	0.644	0	0
SPP1	3.69	0.6	0	0
APOC1	3.48	0.612	0.003	0
MT1G	3.16	0.419	0.003	1.00E−195
MT2A	3.05	0.712	0.306	3.92E−158
C15orf48	2.98	0.769	0.021	0
MT1X	2.91	0.548	0.137	2.81E−144
C1QB	2.70	0.377	0.009	4.31E−163
HSPB1	2.68	0.757	0.152	3.60E−284
C1QA	2.46	0.412	0.047	2.88E−139
MT1H	2.44	0.212	0	5.17E−92
CCL2	2.40	0.352	0.004	8.20E−157
TIMP1	2.38	0.866	0.625	1.37E−138
HLA-DRB5	2.35	0.856	0.185	0
G0S2	2.30	0.54	0.158	1.98E−114
C1QC	2.20	0.364	0.002	1.02E−166
MT1E	2.10	0.393	0.004	5.70E−179
HSPA1A	2.06	0.652	0.24	1.18E−148
HSPA1B	2.0	0.533	0.022	4.02E−238

FC, fold change; FSGS, focal segmental glomerular sclerosis; P_val_adj, adjusted *P* value; PBMC, peripheral blood mononuclear cell.
The peripheral blood monocyte data are from 10x Genomics PBMC version 2 with approximately 8000 cells. Genes are ordered in descending expression levels, revealed as average log-fold change (natural log) compared with healthy blood monocytes. Fraction.1 and fraction.2 are the fractions of monocytes in urine and peripheral blood, respectively, that express mRNA for particular genes.

We performed gene ontology pathway analysis for each cell cluster, and details can be found in Supplementary Note S4 and Supplementary Tables S3–S7.

Comparison of FSGS Monocytes With Healthy PBMC Monocytes

Because monocytes were the major immune cell type in FSGS urine, we compared all urine monocytes with peripheral blood monocyte data available from 10x Genomics (PBMC 8k data set in v2 chemistry). We found that the most highly expressed genes in both MC1 and MC2 were up-regulated when compared with PBMC monocytes, in which many of these genes were expressed in only a small fraction of cells (Table 2 and Figure 2a).

To further characterize the subpopulations of these monocytes and their activated states, we performed pseudotime analysis by combining FSGS monocytes and PBMC monocytes. This analysis revealed 3 branches of cells (Figure 2b), with all PBMC monocytes concentrated at the terminal of branch 2 and FSGS monocytes diverging into branches 1 and 3 (Supplementary Figure S7). We evaluated the branch-specific gene expression and found that FSGS monocytes in branch 1 had up-regulation of the top genes in MC1 (*TIMP1*, *CCL2*, *IL1B*) and those in branch 3 displayed up-regulation of the top genes in MC2 (*APOE*, *APOC1*, *C1QB*) (Figure 2c).

As the monocytes in branch 1 express *IL1B* and *CCL2*, which are characteristic M1 genes, and those in branch 3 express characteristic M2 genes, such as *CD163*, *MRC1*, and *VSIG4* (Figures 2d and e), we hypothesized that these 2 branches represent M1 and M2 monocyte populations. We confirmed the results from pseudotime analysis using monocyte data from a different healthy PBMC data set from 10x Genomics (PBMC 4k v2 chemistry), with high rates of overlap in M1- and M2-specific gene lists (Supplementary Figure S8 and Supplementary Table S11).

We also annotated the urine single-cell data with Blueprint and Encode reference data. Using these data sets, we found that MC1 expression was more aligned with an M1 signature and the MC2 expression was more aligned with an M2 signature (Figure 2f). We also evaluated the enrichment of different immune signatures using the gene lists from Azizi *et al.*[15] The MC2 cluster had the strongest enrichment for an M2 signature (Figure 2g). Consistent with the positivity of dendritic cell marker genes, the MC3 cluster had dendritic cell signature enrichment with Blueprint and Encode annotation and strong enrichment of M1 and anti-inflammatory immune signatures (Figure 2f and g), suggesting monocytes in these clusters were differentiating into inflammatory dendritic cells.

We next evaluated the expression of *PLAUR*, which encodes soluble urokinase plasminogen activator receptor, a circulating factor implicated in FSGS pathogenesis,[16] in the urine single-cell data. *PLAUR* expression was the highest in the MCs, compared with other urine cell clusters. We also evaluated *PLAUR* expression in the single-cell data from the Humphreys

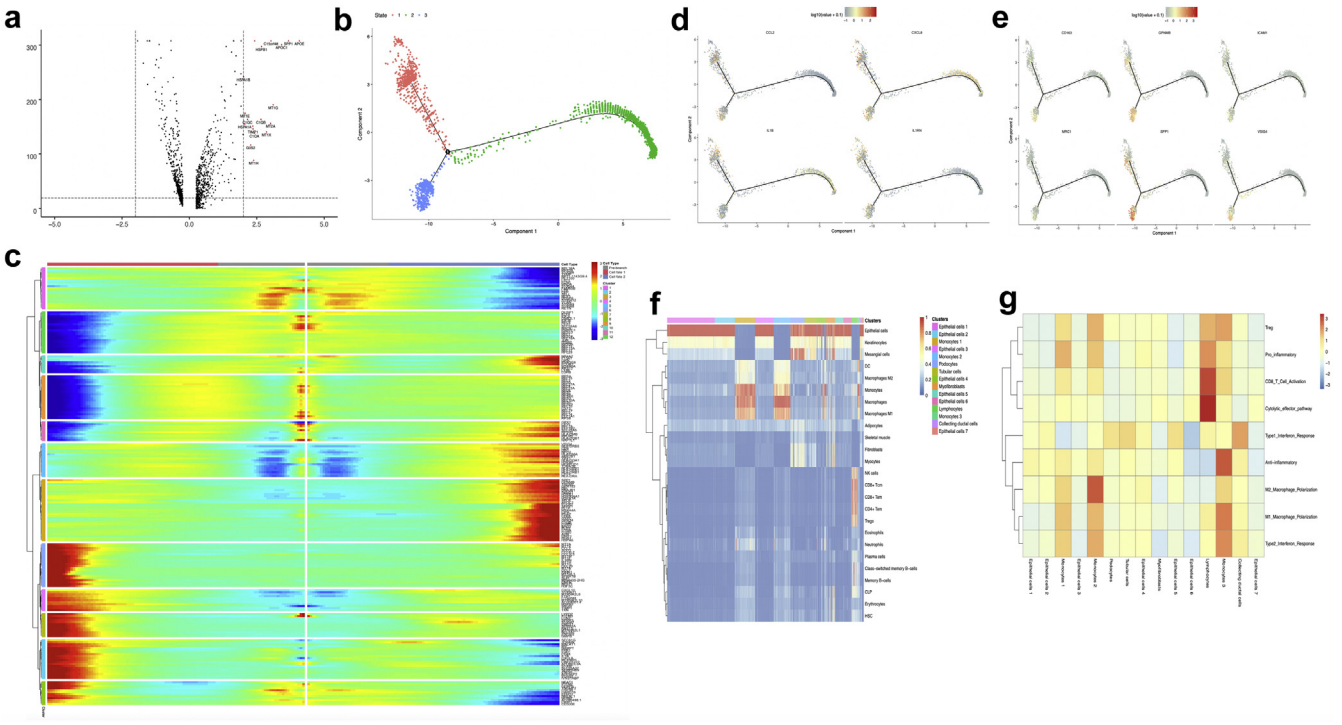

Figure 2. Molecular characterization of urine monocytes from subjects with FSGS. (a) Volcano plot revealing the up-regulated and down-regulated genes in FSGS monocytes compared with healthy PBMC monocytes. Red dots reveal genes with log fold change > 2. (b) Pseudotime trajectory analysis of combined FSGS and peripheral blood monocytes from a healthy volunteer (10× PBMC 8k data set). Trajectory analysis reveals a branching point, connecting 3 cell states. Healthy peripheral blood monocytes are all in state 2 (green) as illustrated in Supplementary Figure S7. (c) Expression heatmap of these 3 states (branches), considering peripheral blood monocytes as the naive state (prebranch). Each horizontal line represents 1 gene and the vertical lines represent all 2946 monocytes (1040 from urine of 12 subjects with FSGS and 1904 from peripheral blood of 1 healthy donor). Expression level is color coded, from red (high) to blue (low). Only genes with $P < 10^{-20}$ are illustrated. (d) Expression of canonical M1 monocyte marker genes in pseudotime branches. (e) Expression of canonical M2 monocyte marker genes in pseudotime branches. (f) Urine single-cell data were annotated using the SingleR R-package and Blueprint and Encode reference data (transcriptional data for various cell types). In this matrix, each vertical line represents 1 urine cell and the horizontal lines represent comparisons to signatures of 25 most closely matched cell types, as labelled on the right. Blue denotes low enrichment and red denotes high enrichment for the characteristic cell signature as labelled. (g) We looked for enrichment of immune signatures using gene lists from Azizi *et al.*[15] The X-axis illustrates 15 cell clusters and Y-axis illustrates 9 immune functions. Collective gene signatures are illustrated as colors representing relative expressions, with red color representing the highest expression. The M1 cluster is modestly enriched for M1 polarization and proinflammatory gene expression. The M2 cluster is strongly enriched for M2 polarization and the M3 cluster is enriched for M1 polarization, and surprisingly, anti-inflammatory pathways. The lymphocyte cluster is enriched for CD8 T cell activation and cytolytic effector pathway genes. FSGS, focal segmental glomerular sclerosis; k, thousand; PBMC, peripheral blood mononuclear cell.

Laboratory, Washington University. There, we observed that *PLAUR* was highly expressed only in the MCs found in kidney allograft rejection data,[17] and in contrast, relatively low expression was observed in the normal kidney tissue (Supplementary Figure S9).[18] Taken together, these data suggest that under these conditions, kidney inflammation is characterized by increased monocyte *PLAUR* expression.

Cell-to-Cell Interactions

To identify potential cell-cell interactions occurring among the various immune and renal epithelial cell types, we used CellPhoneDB,[2,3] (www.cellphonedb.org) which makes statistical inferences based on expression of ligands and the cognate receptors (Figure 3a–c). There were potential interactions between immune and renal epithelial cells involving cytokines from TNF family and TGFB1, including interleukin-1β signaling (Figure 3a), and between lymphocytes and monocytes involving CCL5 (Figure 3b), which is a chemokine secreted by cytotoxic lymphocytes and plays an active role in recruiting leukocytes into inflammatory sites.

Notably, of the TNF family cytokines, the most prominent potential interaction was TNFSF12 (TWEAK) and TNFRSF12A (Fn14) between the immune cells and kidney epithelial cells. Other potential interactions were TNFSF10 (TRAIL) with TNFRSF10B (DR5) and with TNFRSF11B (osteoprotegerin) receptors and TNF with TNFRSF1A and TNFRSF1B receptors.

Immune and EMT Gene Signature Differences Between FSGS and MCD

As we detected immune cells in the urine of the subjects with FSGS, we hypothesized that their infiltration

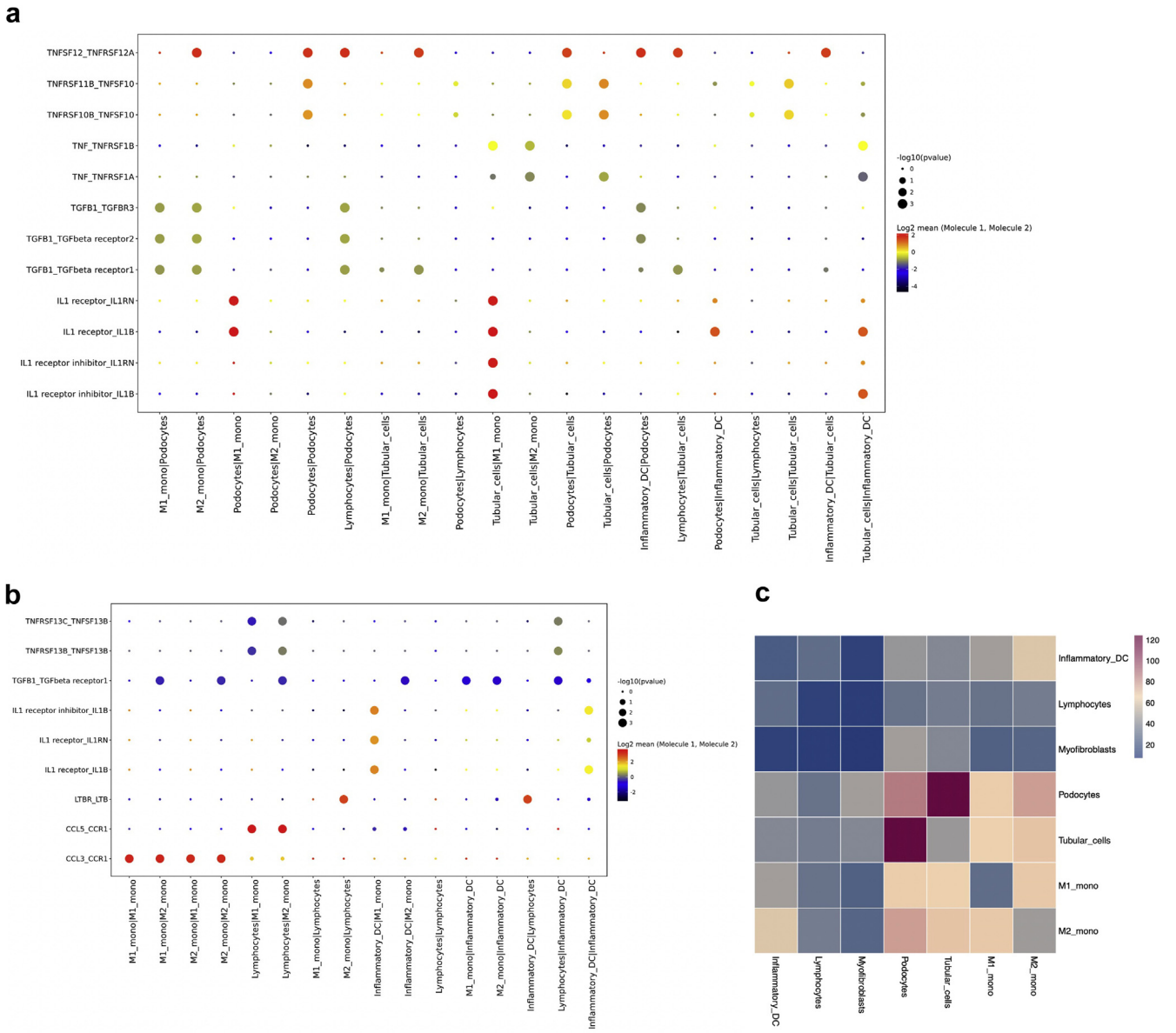

Figure 3. Cell-cell interactions of ligands and receptors between different clusters of urine cells. (a) Dot plot revealing selected interactions between immune cell clusters and renal epithelial cell clusters. (b) Dot plot revealing selected interactions between immune cell clusters (c) Heatmap revealing the number of all the interactions between the urine single-cell clusters. IL, interleukin.

into the kidneys is important for the development and progression of FSGS. Consequently, we sought to evaluate whether the presence of these immune cells would distinguish FSGS from MCD. To this end, we selected the 16 most highly expressed genes identified in the immune cells (8 from monocytes and 8 from lymphocytes), based on their log-fold changes and specificity of expression in these cell types (Supplementary Figure S10 and Supplementary Table S12). We also confirmed the specificity of these genes for immune cells in single-nuclear RNA-seq data from human adult kidney tissue, as reported by Menon *et al.*[19] (Supplementary Figure S11).

We compared expression of these 16 highly expressed genes between FSGS and MCD cases in kidney transcriptomic data from the NEPTUNE study.[20] Compared with MCD, FSGS samples had higher expression levels of these 16 genes and the difference was more profound in the tubulointerstitial compartment (Wilcoxon P value, 1.37×10^{-6}). Importantly, this tubulointerstitial immune profile was also more significant when distinguishing subjects with nephrotic syndrome (FSGS, MCD, and membranous nephropathy), with complete remission from similar subjects without remission. Nonremitting samples had higher expression of these immune genes (Wilcoxon P value $= 1.52 \times 10^{-4}$) (Figure 4a–h).

We next evaluated whether the EMT signature was different between FSGS and MCD samples. The glomerular expression profile of the 10 most highly

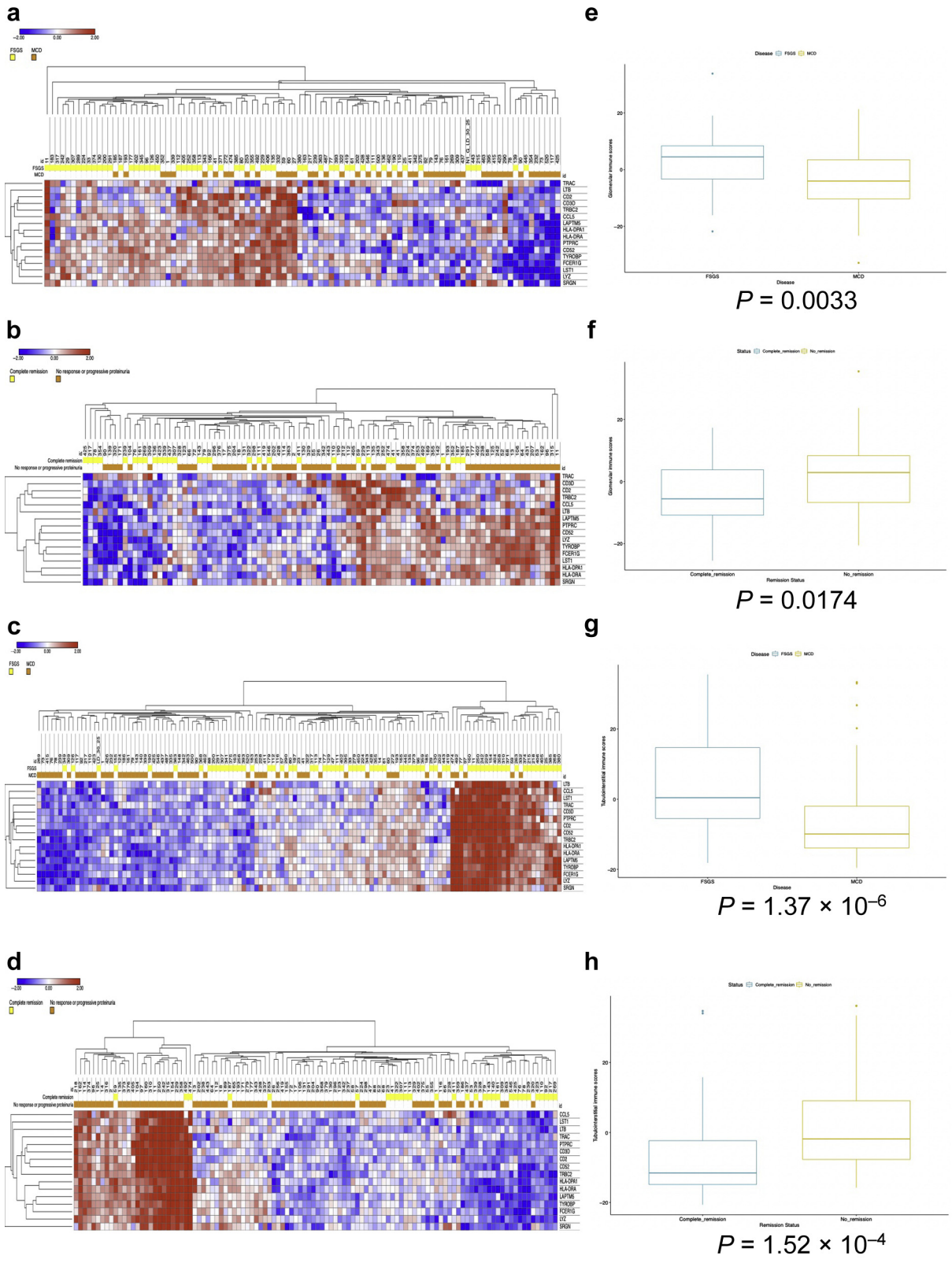

Figure 4. Heatmaps and box plots revealing the expression of the 16 most highly expressed genes from monocyte and lymphocyte clusters in the transcriptomic data from NEPTUNE cohort. (a–d) Heatmaps revealing (a) glomerular expression of MCD ($n = 47$) and FSGS ($n = 51$) samples; (b) glomerular expression of nephrotic syndrome samples (FSGS, MCD, and MN) with subsequent complete remission ($n = 31$) and samples without subsequent remission (no response or progressive proteinuria) ($n = 65$); (c) tubulointerstitial expression of MCD ($n = 55$) and FSGS ($n = 68$) samples; (d) tubulointerstitial expression of nephrotic syndrome samples with complete remission ($n = 30$) and samples without remission ($n = 80$). (e–h) Box plots revealing combined expression Z-scores of 16 genes in (e) glomerular expression data of MCD and FSGS samples; (f) glomerular expression data of all nephrotic syndrome samples with complete remission and samples without remission; (g) tubulointerstitial expression data of MCD and FSGS samples; (h) tubulointerstitial expression of all nephrotic syndrome samples with complete (continued)

expressed EMT-related genes in podocytes (Supplementary Table S13) revealed significant difference between the 2 diseases, with FSGS samples having higher EMT signature. The Wilcoxon tests comparing the combined EMT signature scores between these 2 diseases were significant in both the glomerular compartment (Wilcoxon P value $= 2.0 \times 10^{-4}$) and the tubulointerstitial compartment (Wilcoxon P value $= 3.35 \times 10^{-5}$) (Figure 5a–d).

Immune Signatures in Lupus Nephritis

To evaluate the commonality of immune marker gene expression and their potential utility in other glomerular diseases, we evaluated their expression in the immune single-cell data from the subjects with lupus nephritis in the Accelerating Medicines Partnership,[21] as reported by Arazi *et al.*[22] We observed that the top 16 immune marker genes from FSGS monocytes and lymphocytes were also highly expressed in the monocyte and lymphocyte clusters, respectively, from subjects with lupus nephritis (Figure 6a and b). We also evaluated the expression of these immune genes in the bulk RNA-seq data of urine samples from another multiethnic cohort of subjects with lupus nephritis and found that subjects with active disease (defined as urine protein-to-creatinine ratio > 0.5) had higher expression of these genes than those with inactive disease (urine protein-to-creatinine ratio ≤ 0.5), reflecting the higher presence of monocytes/lymphocytes in the urine of subjects with active lupus nephritis (Figure 6g).

Finally, we investigated the gene expression related to M1 and M2 signatures from the pseudotime heatmap (Figure 2c) in the Accelerating Medicines Partnership kidney immune single-cell data of lupus nephritis. The M1 signature genes were enriched in the myeloid cell heatmap clusters, especially in the inflammatory and phagocytic $CD16^+$ macrophages (CM0 and CM1), and M2 signature genes were found to be more enriched in tissue resident macrophages, conventional dendritic cells, and M2-like $CD16^+$ macrophages (CM2, CM3, and CM4) (Figures 6c–f).

DISCUSSION

In this study, we report scRNA-seq results of urine cells from subjects with FSGS. Our findings revealed a landscape of immune cells, podocytes, myofibroblasts, and tubular cells with distinct expression profiles. We used canonical marker genes to identify the major cell types and confirmed those identifications by annotation using Encode and Blueprint transcriptional reference data.

Urine podocytes had loss of canonical podocyte markers, such as *NPHS1*, *NPHS2*, and *PODXL*, and high expression of EMT markers. The protein products of these canonical podocyte genes are essential for the proper podocyte function. In cell culture, human and mouse podocytes also lose expression of NPHS1 and NPHS2,[23,24] and this down-regulation or loss in FSGS urinary podocytes could be due to podocyte injury or dedifferentiation. EMT is important in cancer biology, in which it contributes to increased mobility of cancer cells. Podocytes may undergo a form of nonmalignant EMT,[25,26] leading to loss of differentiated function and possibly loss of cells in the urinary space.

The podocyte cluster was also positive for PEC markers, and it is possible to assume that there were some PECs in the podocyte cluster. Nevertheless, PECs are also known to undergo EMT, and these markers are reported to be involved in the EMT process,[27–31], making it difficult to confirm the presence of PECs in the current study.

The presence of myofibroblasts in the urine from cases with FSGS suggests that the kidney cells are undergoing EMT and that it may contribute to glomerulosclerosis and tubulointerstitial fibrosis. This is in part supported by annotation using Encode and Blueprint reference transcriptomic data, in which the podocyte and tubular cell clusters had transcriptional similarities with myocytes and fibroblasts (Figure 2f) and the higher EMT signature scores in samples with FSGS from the NEPTUNE cohort. Tubular epithelial cell EMT has been proposed to contribute to tubulointerstitial fibrosis in chronic kidney disease,[32–34] consistent with our finding of higher EMT gene expression in the samples with FSGS compared with those with MCD.

There were immune cells, predominantly monocytes, in the FSGS urine samples, and we identified monocyte subtypes and characterized their gene expression profiles. Monocytes and/or macrophages expressing *APOE*, *APOC1*, and *SPP1* have been reported in single-cell studies of Alzheimer disease,[35] atherosclerosis,[36] and breast cancer.[15] These cells were considered to be foam cells owing to their high expression of lipoproteins (*APOE* and *APOC1*). In pseudotime analysis, we found that the FSGS monocytes constituted 2 branches, one with M1

Figure 4. (continued) remission and samples without remission. The P values for Z-score comparisons were by two-sided Wilcoxon tests. In the box plots, center line is the median, box limits are upper and lower quartiles, whiskers are 1.5× interquartile range, and the points represent outliers. FSGS, focal segmental glomerular sclerosis; MCD, minimal change disease; MN, membranous nephropathy; NEPTUNE, The Nephrotic Syndrome Study Network.

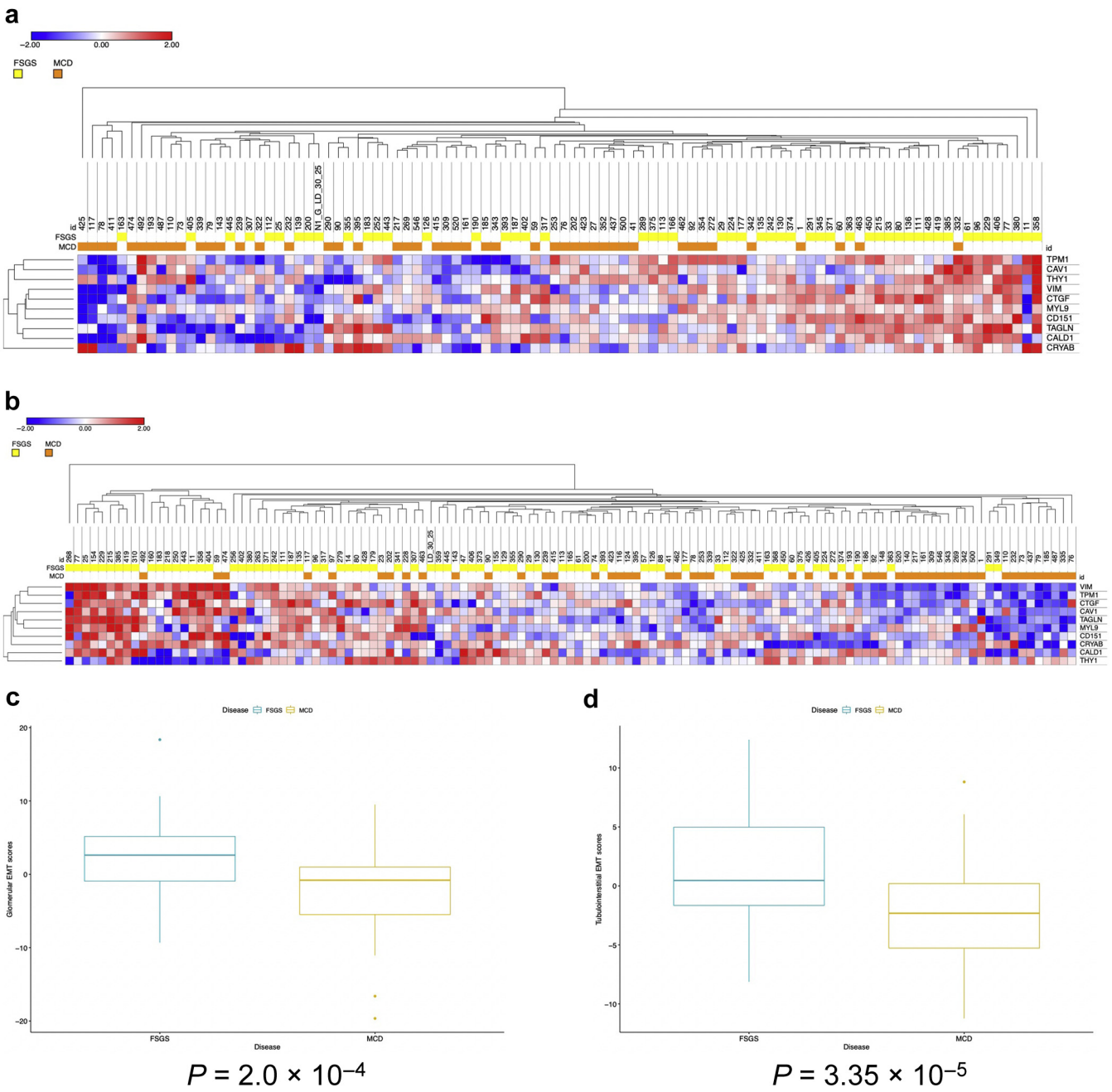

Figure 5. Heatmaps and box plots revealing the expression of the 10 selected EMT genes in the transcriptomic data from NEPTUNE cohort. (a) Heatmap revealing glomerular expression of MCD ($n = 47$) and FSGS ($n = 51$) samples. (b) Heatmap revealing tubulointerstitial expression of MCD ($n = 55$) and FSGS ($n = 68$) samples. (c) Box plot revealing combined Z-scores of 10 EMT genes in glomerular expression data of MCD and FSGS samples. (d) Box plot revealing combined Z-scores of 10 EMT genes in tubulointerstitial expression data of MCD and FSGS samples. The *P* values for Z-score comparisons were by two-sided Wilcoxon tests. In the box plots, center line is the median, box limits are upper and lower quartiles, whiskers are 1.5× interquartile range, and the points represent outliers. EMT, epithelial-mesenchymal transition; FSGS, focal segmental glomerular sclerosis; MCD, minimal change disease; NEPTUNE, The Nephrotic Syndrome Study Network.

characteristics (*TIMP1*, *IL1B* expression) and the other with M2 features (*APOE*, *APOC1* expression). The urinary M1- and M2-related signature genes from the pseudotime analysis were also highly expressed in myeloid subpopulations of kidney immune cells from lupus nephritis. This shared pattern across diverse diseases reveals that these inflammatory macrophage expression signatures are common across inflammatory conditions. We also found MC with features of inflammatory dendritic cells. These cells are known to be involved in the initiation and maintenance of TH17 cell response, which has been implicated in several autoimmune and inflammatory diseases.[37–39]

The inclusion in the present study of multiple samples from the same subjects and subjects with various levels of proteinuria revealed the

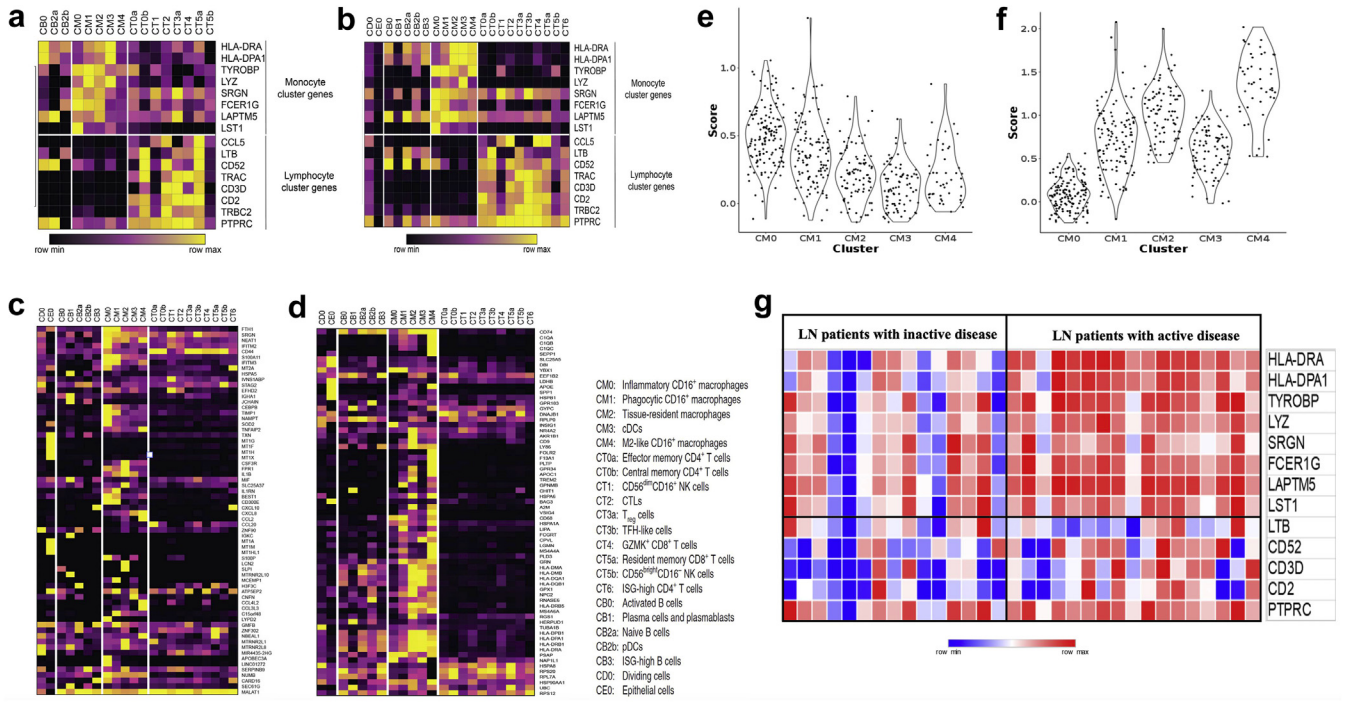

Figure 6. Expression in lupus nephritis data of immune signature genes and monocyte M1 and M2 genes identified from FSGS urine single-cell data. (a, b) Heatmaps revealing the expression of the 16 most highly expressed genes from FSGS monocyte and lymphocyte clusters in the AMP single-cell RNA-seq data of immune cells in lupus nephritis from (a) urine samples and (b) kidney biopsy samples (c, d). Heatmaps revealing the expression of (c) M1- and (d) M2-specific monocyte genes as illustrated in Figure 2c in the AMP single-cell RNA-seq data of immune cells from lupus nephritis kidney biopsy samples. (e) Violin plot of M1 scores, calculated as the average-scaled expression of M1 genes in Figure 6c, in myeloid cell clusters in AMP lupus nephritis data. (f) Violin plot of M2 scores from M2 genes in Figure 6d in the same lupus nephritis data. (g) Heatmap revealing the expression of the most highly expressed monocyte and lymphocyte markers in the urine bulk RNA-seq data of patients with lupus nephritis with active and inactive diseases. AMP, Accelerating Medicines Partnership; FSGS, focal segmental glomerular sclerosis; RNA-seq, RNA sequencing.

reproducibility of the cell-capturing and analysis pipelines. We looked for the variability in the cell numbers of selected cell types among the samples from subject 1 and found that 2 cell samples coming from 1 urine sample (US_03) to have relatively fewer cells (Supplementary Table S14). Nevertheless, the proteinuria level at the time of that urine sample collection for this sample was not considerably different from values at other times of sample collections (Supplementary Table S15), and the low cell counts could possibly be due to a smaller urine volume in that sample and/or a likely increase in loss of cells during sample preparation and handling.

Expression of genes specifically enriched in urinary MCs could contribute to podocyte injury and/or could serve as biomarkers to detect ongoing podocyte injury. We found that inflammatory monocytes expressed high levels of *PLAUR* (encoding soluble urokinase plasminogen activator receptor). These monocytes could, therefore, be a source of plasma and urinary soluble urokinase plasminogen activator receptor, which has been implicated in FSGS pathogenesis. *APOE* was the most significantly up-regulated gene in FSGS monocytes when compared with peripheral blood monocytes from a healthy individual. Serum and urine levels of *APOE* are elevated in FSGS and nephrotic syndrome.[40] Other most highly up-regulated genes in FSGS monocytes included *SPP1* (encoding the immune modulator, osteopontin), *APOC1*, and several metallothionein genes (*MT1G*, *MT2A*, *MT1X*, *MT1H*, *MT1E*, among others). Osteopontin is up-regulated in several autoimmune and inflammatory diseases, including rheumatoid arthritis, multiple sclerosis, Crohn's disease, cancers, and atherosclerosis; targeting osteopontin by monoclonal antibodies in rheumatoid arthritis primate models ameliorated the symptoms, suggesting a possible role in pathogenesis.[41]

On the basis of the FSGS single-cell data, we evaluated expression of immune and EMT genes in the NEPTUNE transcriptomic data. This analysis was informative for 3 reasons. First, NEPTUNE provided validation of the present findings in a larger cohort of different sample type (kidney biopsy) and technology (microarray data). Second, the NEPTUNE cohort contains gene expression data from MCD biopsies, and this served as a disease comparator for FSGS. Third, it enabled us to correlate our gene expression data with nephrotic disease remission in this cohort.

The expression levels of immune genes were higher in FSGS than in MCD samples and was also higher in subjects with nephrotic proteinuria without remission compared with those in complete remission. Similarly, the higher immune signature in the urine of subjects with active lupus nephritis reflects the presence of higher number of immune cells. These findings suggest the potential use of these marker genes to monitor disease activity.

In the NEPTUNE data, both glomerular expression and tubulointerstitial expression of the EMT genes were also higher in FSGS compared with MCD samples, likely reflecting the cell injury and fibrotic changes in FSGS, which are typically absent in MCD. Because the NEPTUNE EMT signature is from bulk expression data, the glomerular EMT signature may also be contributed by PECs, which can also undergo EMT, as found in the setting of glomerulonephritis.[42–44] The combined immune and EMT signatures represent the profibrotic expression profile that distinguishes FSGS from MCD and could be associated with progressive fibrosis and renal function decline.

EMT is known to be induced in part by M2 monocytes through TGF-β signaling.[45,46] Cell-to-cell interaction analysis suggested *TGFB1* signaling between kidney epithelial cells and all immune cell types. It also revealed signaling of cytokines from the TNF family. Recently, a study using the transcriptomic data from NEPTUNE and the European Renal cDNA Bank identified high TNF activation signatures in a subset of nephrotic syndrome samples with predominantly (∼80%) FSGS cases. These subjects had a higher risk of disease progression compared with other groups with low TNF signatures.[47] Previously, treatment of patients with therapy-resistant FSGS with adalimumab in the FONT trial (novel therapies in resistant FSGS) was unsuccessful, with only 2 patients having dramatic improvement in proteinuria level (from 17 to 0.6 mg/mg and from 3.6 to 0.6 mg/mg).[47,48] Cell-cell interaction results from the current study also revealed that TNFSF12-TNFRSF12A (TWEAK/Fn14) and TNFSF10-TNFRSF10B (TRAIL/DR5) interactions are stronger than the TNF interactions. Both TWEAK and TRAIL are known to induce apoptosis and are implicated in chronic inflammation, organ remodeling, and fibrosis; these could be potential therapeutic targets.[49–56]

In a recent urine single-cell RNA-seq study of subjects with diabetic kidney disease, Abedini *et al*.[57] were able to identify various immune and kidney epithelial cells. In another single-cell study of lupus nephritis, Arazi *et al*.[22] also observed high correlation of expression profiles between leukocytes in the urine and those in the kidney biopsy, suggesting the potential role of urinary cellular biomarkers in lupus nephritis. In the present study, scRNA-seq captured the expression landscape of renal epithelial cells undergoing EMT in the urine, which reflects the renal pathology of patients with FSGS. Urothelial cells, which are not known to be mechanistically involved in the FSGS pathogenesis, were not analyzed in detail, owing in part to the difficulties assigning tissue specific markers to the relevant clusters.

This study has several limitations. Owing to the limited number of urine single-cell samples and lack of healthy or subjects with MCD, we could not evaluate the diagnostic and prognostic potential of urine immune cells for FSGS. Studies with larger sample sizes will be needed to capture immune cells in the urine, possibly by fluorescence-activated cell sorting to determine the sensitivity and specificity of this approach in distinguishing FSGS from MCD. Similarly, in future studies, it might be possible to quantify the protein products of some of the inflammatory genes from monocytes in the serum and urine by enzyme-linked immunosorbent assay or other approaches to be evaluated for diagnostic and prognostic potential.

In summary, this study describes in detail the transcriptional profile of various cell types that are present in the urine of subjects with FSGS and provides insights into relevant pathophysiologic processes. These findings suggest the possibility of using urine as liquid biopsy and propose potential biomarkers and therapeutic targets for further exploration.

DISCLOSURE

All the authors declared no competing interests.

ACKNOWLEDGMENTS

This work was supported by the Intramural Research Program of the National Institute of Diabetes and Digestive and Kidney Diseases, National Institutes of Health, Bethesda, Maryland (institutional review board protocols: 94-DK-0127—Pathogenesis of Glomerulosclerosis; 94-DK-0133—Focal Segmental Glomerulosclerosis Genetics) (principal investor JBK) and the National Institutes of Health bench to bedside grant R01-DK108368-04S1 (principal investors JBK, CAW, KS, GHG, BLL, PER, and MMM). Support from CCR Single Cell Analysis Facility was funded by FNLCR Contract HHSN261200800001E, and support from Michigan Medicine was funded by O'Brien Kidney Research Core Center P30DK081943 (principal investor Matthias Kretzler). The Nephrotic Syndrome Study Network Consortium (NEPTUNE), U54-DK-083912, is a part of the National Institutes of Health Rare Disease Clinical Research Network, supported through a collaboration between the Office of Rare Diseases Research, National Center for Advancing Translational Sciences and the National Institute of Diabetes and Digestive and Kidney Diseases. Additional funding and/or programmatic support

for this project has also been provided by the University of Michigan, the NephCure Kidney International, and the Halpin Foundation. We thank Boehringer Ingelheim for supporting the establishment of the METAPHOR (Multi-EThnic American luPus coHORt) lupus nephritis cohort. We thank Bao Tran, Jyoti Shetty, and other members of the CCR-Sequencing Facility for their help with the sequencing; Pradeep Kumar Dagur and Phil McCoy for their help with the fluorescence-activated cell sorting experiments; Elizabeth Binns-Roemer and Mary Thompson for technical support; Luis Fernando Menezes for critical manuscript review; and Jodi Blake, Badryah Omar, Noor Khalil, and Tina Mainieri for helping with sample collection and data retrieval.

AUTHOR CONTRIBUTIONS

JBK, CAW, KS, DSR, GHG, BLL, PER, and MMM conceived the study. JH designed the experiments. JH, JHJ, and KZL performed the experiments. MCK helped with single-cell capture. MM and PK helped with the single-cell capture and next-generation sequencing. KZL, JH, and JHJ performed the data analysis. KS, YZ, VC, GWN, and MC gave advice on data analysis. GWN performed back-calculation of batch-corrected expression levels. CCB, SE, and MK provided NEPTUNE transcriptomic data. CCB and AA performed the analysis of lupus nephritis data. JBK, KS, CAW, DSR, RRS, GHG, BLL, PER, MMM, KZL, JH, AZR, MK, and TY interpreted the results. KZL drafted the manuscript and all authors approved the final manuscript.

SUPPLEMENTARY MATERIAL

Supplementary File (PDF)

Note S1. Members of the Nephrotic Syndrome Study Network (NEPTUNE).

Note S2. Calculating batch-corrected gene expression levels from Harmony-corrected principal components.

Note S3. Analysis using one sample per subject.

Note S4. Pathway analysis of podocyte, monocyte, and lymphocyte clusters.

Supplementary Methods.

Figure S1. Stackplots revealing the number of cells per cell type category.

Figure S2. t-SNE and violin plots revealing expression of canonical marker genes for leukocytes, renal epithelial, and urothelial cells.

Figure S3. t-SNE plots revealing expression of markers for PECs.

Figure S4. Expression profiles of dendritic cell marker genes in the urine scRNA-seq data.

Figure S5. PCs calculated from back-calculated expression levels preserve the Harmony batch correction.

Figure S6. t-SNE plots colored by back-calculated gene expression levels, for comparison with gene expression levels found in Supplementary Figure S1.

Figure S7. Trajectory plot of monocytes revealing the original samples of the cells.

Figure S8. Pseudotime trajectory analysis of combined FSGS and peripheral blood monocytes from a healthy volunteer (10x PBMC 4k data set).

Figure S9. High expression of PLAUR (encoding suPAR) found in monocyte clusters.

Figure S10. Violin plots revealing the most highly expressed monocyte/lymphocyte marker genes that were used to interrogate the presence of immune cells in the NEPTUNE transcriptomic data.

Figure S11. Violin plots revealing the most highly expressed monocyte/lymphocyte marker genes in the single nuclear RNAseq data from human adult kidney tissue from Menon et al.

Figure S12. Stackplots revealing cell population (%) by covariates.

Figure S13. Overview of the experiments and analysis of the urine single-cell study.

Figure S14. Violin plots revealing (A) number of genes, (B) number of unique molecular identifiers, and (C) mitochondrial percentage of individual clusters in the urine FSGS single-cell data set.

Table S1. The percentage of cells from each subject contributing to different cell clusters in the FSGS urine scRNA-seq study.

Table S2. The most highly expressed genes in podocyte cluster compared with remaining clusters.

Table S3. Gene ontology pathway analysis of the most highly expressed genes (log FC $>=$ 1) from podocyte cluster (n $=$ 38).

Table S4. The most highly expressed genes in monocyte clusters compared with remaining clusters.

Table S5. Gene ontology pathway analysis of significant genes from monocyte clusters (n $=$ 817).

Table S6. The most highly expressed genes in lymphocyte cluster compared with remaining clusters.

Table S7. Gene ontology pathway analysis of significant genes from lymphocyte cluster (n $=$ 481).

Table S8. The most highly expressed genes in podocyte cluster in the analysis of seven samples, each from a single subject with urinary protein to creatinine ratio $>$ 0.5.

Table S9. The most highly expressed genes in monocyte cluster in the analysis of seven samples, each from a single subject with urinary protein to creatinine ratio $>$ 0.5.

Table S10. The most highly expressed genes in lymphocyte cluster in the analysis of seven samples, each from a single subject with urinary protein to creatinine ratio $>$ 0.5.

Table S11. The overlap of M1- and M2-specific gene lists from the pseudotime heatmaps using PBMC 8k and 4k monocytes.

Table S12. The 16 most highly expressed genes from monocyte and lymphocyte clusters selected to be evaluated in the NEPTUNE kidney transcriptomic data.

Table S13. Ten genes from the podocyte cluster reported to be associated with EMT.

Table S14. The breakdown of the important cell types for each of the cell samples from subject 1.

Table S15. Proteinuria, creatinine, and eGFR values measured at the time of collection of urine samples for subject 1.

Table S16. Statistics of the cell counts, barcodes, reads, genes, and UMIs for each sample.

REFERENCES

1. Mak SK, Short CD, Mallick NP. Long-term outcome of adult-onset minimal-change nephropathy. *Nephrol Dial Transplant*. 1996;11:2192–2201. https://doi.org/10.1093/oxfordjournals.ndt.a027136
2. Waldman M, Crew RJ, Valeri A, et al. Adult minimal-change disease: clinical characteristics, treatment, and outcomes. *Clin J Am Soc Nephrol*. 2007;2:445–453. https://doi.org/10.2215/CJN.03531006
3. Park J, Liu C, Kim J, Susztak K. Understanding the kidney one cell at a time. *Kidney Int*. 2019;96:862–870. https://doi.org/10.1016/j.kint.2019.03.035
4. Park J, Shrestha R, Qiu C, et al. Single-cell transcriptomics of the mouse kidney reveals potential cellular targets of kidney disease. *Science*. 2018;360:758–763. https://doi.org/10.1126/science.aar2131
5. Wilson PC, Humphreys BD. Kidney and organoid single-cell transcriptomics: the end of the beginning. *Pediatr Nephrol*. 2020;35:191–197. https://doi.org/10.1007/s00467-018-4177-y
6. Wu H, Humphreys BD. The promise of single-cell RNA sequencing for kidney disease investigation. *Kidney Int*. 2017;92:1334–1342. https://doi.org/10.1016/j.kint.2017.06.033
7. Butler A, Hoffman P, Smibert P, Papalexi E, Satija R. Integrating single-cell transcriptomic data across different conditions, technologies, and species. *Nat Biotechnol*. 2018;36:411–420. https://doi.org/10.1038/nbt.4096
8. Korsunsky I, Millard N, Fan J, et al. Fast, sensitive and accurate integration of single-cell data with Harmony. *Nat Methods*. 2019;16:1289–1296. https://doi.org/10.1038/s41592-019-0619-0
9. Qiu X, Mao Q, Tang Y, et al. Reversed graph embedding resolves complex single-cell trajectories. *Nat Methods*. 2017;14:979–982. https://doi.org/10.1038/nmeth.4402
10. Efremova M, Vento-Tormo M, Teichmann S, Vento-Tormo R. CellPhoneDB: inferring cell-cell communication from combined expression of multi-subunit receptor-ligand complexes. *Nat Protoc*. 2020;15:1484–1506. https://doi.org/10.1038/s41596-020-0292-x
11. Vento-Tormo R, Efremova M, Botting RA, et al. Single-cell reconstruction of the early maternal-fetal interface in humans. *Nature*. 2018;563:347–353. https://doi.org/10.1038/s41586-018-0698-6
12. Matsumoto T, Hess S, Kajiyama H, et al. Proteomic analysis identifies insulin-like growth factor-binding protein-related protein-1 as a podocyte product. *Am J Physiol Ren Physiol*. 2010;299:F776–F784. https://doi.org/10.1152/ajprenal.00597.2009
13. Zhang J, Liu J, Wu J, Li W, Chen Z, Yang L. Progression of the role of CRYAB in signaling pathways and cancers. *Onco Targets Ther*. 2019;12:4129–4139. https://doi.org/10.2147/OTT.S201799
14. Faure- André G, Vargas P, Yuseff MI, et al. Regulation of dendritic cell migration by CD74, the MHC class II-associated invariant chain. *Science*. 2008;322:1705–1710. https://doi.org/10.1126/science.1159894
15. Azizi E, Carr AJ, Plitas G, et al. Single-cell map of diverse immune phenotypes in the breast tumor microenvironment. *Cell*. 2018;174:1293–1308.e36. https://doi.org/10.1016/j.cell.2018.05.060
16. Wei C, El Hindi S, Li J, et al. Circulating urokinase receptor as a cause of focal segmental glomerulosclerosis. *Nat Med*. 2011;17:952–960. https://doi.org/10.1038/nm.2411
17. Wu H, Malone AF, Donnelly EL, et al. Single-cell transcriptomics of a human kidney allograft biopsy specimen defines a diverse inflammatory response. *J Am Soc Nephrol*. 2018;29:2069–2080. https://doi.org/10.1681/ASN.2018020125
18. Wu H, Uchimura K, Donnelly EL, Kirita Y, Morris SA, Humphreys BD. Comparative analysis and refinement of human PSC-derived kidney organoid differentiation with single-cell transcriptomics. *Cell Stem Cell*. 2018;23:869–881.e8. https://doi.org/10.1016/j.stem.2018.10.010
19. Menon R, Otto EA, Hoover PJ, et al. Single cell transcriptomics identifies focal segmental glomerulosclerosis remission endothelial biomarker. *JCI Insight*. 2020;5:e133267. https://doi.org/10.1172/jci.insight.133267
20. Gadegbeku CA, Gipson DS, Holzman LB, et al. Design of the Nephrotic Syndrome Study Network (NEPTUNE) to evaluate primary glomerular nephropathy by a multidisciplinary approach. *Kidney Int*. 2013;83:749–756. https://doi.org/10.1038/ki.2012.428
21. Hoover P, Der E, Berthier CC, et al. Accelerating Medicines Partnership: organizational structure and preliminary data from the Phase 1 studies of lupus nephritis. *Arthritis Care Res (Hoboken)*. 2020;72:233–242. https://doi.org/10.1002/acr.24066
22. Arazi A, Rao DA, Berthier CC, et al. The immune cell landscape in kidneys of patients with lupus nephritis. *Nat Immunol*. 2019;20:902–914. https://doi.org/10.1038/s41590-019-0398-x
23. Hagmann H, Brinkkoetter PT. Experimental models to study podocyte biology: Stock-Taking the toolbox of glomerular research. *Front Pediatr*. 2018;6:193. https://doi.org/10.3389/fped.2018.00193
24. Rinschen MM, Schroeter CB, Koehler S, et al. Quantitative deep mapping of the cultured podocyte proteome uncovers shifts in proteostatic mechanisms during differentiation. *Am J Physiol Cell Physiol*. 2016;311:C404–C417. https://doi.org/10.1152/ajpcell.00121.2016
25. Li Y, Kang YS, Dai C, Kiss LP, Wen X, Liu Y. Epithelial-to-mesenchymal transition is a potential pathway leading to podocyte dysfunction and proteinuria. *Am J Pathol*. 2008;172:299–308. https://doi.org/10.2353/ajpath.2008.070057
26. Yamaguchi Y, Iwano M, Suzuki D, et al. Epithelial-mesenchymal transition as a potential explanation for podocyte depletion in diabetic nephropathy. *Am J Kidney Dis*. 2009;54:653–664. https://doi.org/10.1053/j.ajkd.2009.05.009
27. Di Palma T, Lucci V, de Cristofaro T, Filippone MG, Zannini M. A role for PAX8 in the tumorigenic phenotype of ovarian cancer cells. *BMC Cancer*. 2014;14:292. https://doi.org/10.1186/1471-2407-14-292

28. Li L, Wu Y, Yang Y. Paired box 2 induces epithelial-mesenchymal transition in normal renal tubular epithelial cells of rats. *Mol Med Rep*. 2013;7:1549–1554. https://doi.org/10.3892/mmr.2013.1365
29. Lv J, Sun B, Mai Z, Jiang M, Du J. CLDN-1 promoted the epithelial to migration and mesenchymal transition (EMT) in human bronchial epithelial cells via Notch pathway. *Mol Cell Biochem*. 2017;432:91–98. https://doi.org/10.1007/s11010-017-3000-6
30. Ohse T, Pippin JW, Chang AM, et al. The enigmatic parietal epithelial cell is finally getting noticed: a review. *Kidney Int*. 2009;76:1225–1238. https://doi.org/10.1038/ki.2009.386
31. Suh Y, Yoon CH, Kim RK, et al. Claudin-1 induces epithelial-mesenchymal transition through activation of the c-Abl-ERK signaling pathway in human liver cells [published correction appears in *Oncogene*. 2017;36:1167-1168]. *Oncogene*. 2013;32:4873–4882. https://doi.org/10.1038/onc.2012.505
32. Liu Y. Epithelial to mesenchymal transition in renal fibrogenesis: pathologic significance, molecular mechanism, and therapeutic intervention. *J Am Soc Nephrol*. 2004;15:1–12. https://doi.org/10.1097/01.asn.0000106015.29070.e7
33. Ng YY, Huang TP, Yang WC, et al. Tubular epithelial-myofibroblast transdifferentiation in progressive tubulointerstitial fibrosis in 5/6 nephrectomized rats. *Kidney Int*. 1998;54:864–876. https://doi.org/10.1046/j.1523-1755.1998.00076.x
34. Abbate M, Zoja C, Rottoli D, Corna D, Tomasoni S, Remuzzi G. Proximal tubular cells promote fibrogenesis by TGF-beta1-mediated induction of peritubular myofibroblasts [published correction appears in *Kidney Int*. 2002;62:731]. *Kiney Int*. 2002;61:2066–2077. https://doi.org/10.1046/j.1523-1755.2002.00380.x
35. Mathys H, Davila-Velderrain J, Peng Z, et al. Single-cell transcriptomic analysis of Alzheimer's disease. *Nature*. 2019;570:332–337. https://doi.org/10.1038/s41586-019-1195-2
36. Fernandez DM, Rahman AH, Fernandez NF, et al. Single-cell immune landscape of human atherosclerotic plaques. *Nat Med*. 2019;25:1576–1588. https://doi.org/10.1038/s41591-019-0590-4
37. Hu Y, Shen F, Crellin NK, Ouyang W. The IL-17 pathway as a major therapeutic target in autoimmune diseases. *Ann N Y Acad Sci*. 2011;1217:60–76. https://doi.org/10.1111/j.1749-6632.2010.05825.x
38. Segura E, Touzot M, Bohineust A, et al. Human inflammatory dendritic cells induce Th17 cell differentiation. *Immunity*. 2013;38:336–348. https://doi.org/10.1016/j.immuni.2012.10.018
39. Segura E, Amigorena S. Identification of human inflammatory dendritic cells. *Oncoimmunology*. 2013;2:e23851. https://doi.org/10.4161/onci.23851
40. Bruschi M, Catarsi P, Candiano G, et al. Apolipoprotein E in idiopathic nephrotic syndrome and focal segmental glomerulosclerosis. *Kidney Int*. 2003;63:686–695. https://doi.org/10.1046/j.1523-1755.2003.00777.x
41. Lund SA, Giachelli CM, Scatena M. The role of osteopontin in inflammatory processes. *J Cell Commun Signal*. 2009;3:311–322. https://doi.org/10.1007/s12079-009-0068-0
42. Fujigaki Y, Sun DF, Fujimoto T, et al. Mechanisms and kinetics of Bowman's epithelial-myofibroblast transdifferentiation in the formation of glomerular crescents. *Nephron*. 2002;92:203–212. https://doi.org/10.1159/000064469
43. Ng YY, Fan JM, Mu W, et al. Glomerular epithelial-myofibroblast transdifferentiation in the evolution of glomerular crescent formation. *Nephrol Dial Transplant*. 1999;14:2860–2872. https://doi.org/10.1093/ndt/14.12.2860
44. Shimizu M, Kondo S, Urushihara M, et al. Role of integrin-linked kinase in epithelial-mesenchymal transition in crescent formation of experimental glomerulonephritis. *Nephrol Dial Transplant*. 2006;21:2380–2390. https://doi.org/10.1093/ndt/gfl243
45. Yao RR, Li JH, Zhang R, Chen RX, Wang YH. M2-polarized tumor-associated macrophages facilitated migration and epithelial-mesenchymal transition of HCC cells via the TLR4/STAT3 signaling pathway. *World J Surg Oncol*. 2018;16:9. https://doi.org/10.1186/s12957-018-1312-y
46. Zhu L, Fu X, Chen X, Han X, Dong P. M2 macrophages induce EMT through the TGF- β/Smad2 signaling pathway. *Cell Biol Int*. 2017;41:960–968. https://doi.org/10.1002/cbin.10788
47. Mariani LH, Eddy S, Martini S. Redefining nephrotic syndrome in molecular terms: outcome-associated molecular clusters and patient stratification with noninvasive surrogate biomarkers. *bioRxiv*. 2018. https://doi.org/10.1101/427880.
48. Joy MS, Gipson DS, Powell L, et al. Phase 1 trial of adalimumab in focal segmental glomerulosclerosis (FSGS): II. Report of the FONT (Novel Therapies for Resistant FSGS) study group. *Am J Kidney Dis*. 2010;55:50–60. https://doi.org/10.1053/j.ajkd.2009.08.019
49. Burkly LC. TWEAK/Fn14 axis: the current paradigm of tissue injury-inducible function in the midst of complexities. *Semin Immunol*. 2014;26:229–236. https://doi.org/10.1016/j.smim.2014.02.006
50. Burkly LC, Michaelson JS, Hahm K, Jakubowski A, Zheng TS. TWEAKing tissue remodeling by a multifunctional cytokine: role of TWEAK/Fn14 pathway in health and disease. *Cytokine*. 2007;40:1–16. https://doi.org/10.1016/j.cyto.2007.09.007
51. Ucero AC, Benito-Martin A, Fuentes-Calvo I, et al. TNF-related weak inducer of apoptosis (TWEAK) promotes kidney fibrosis and Ras-dependent proliferation of cultured renal fibroblast. *Biochim Biophys Acta*. 2013;1832:1744–1755. https://doi.org/10.1016/j.bbadis.2013.05.032
52. Wynn TA, Ramalingam TR. Mechanisms of fibrosis: therapeutic translation for fibrotic disease. *Nat Med*. 2012;18:1028–1040. https://doi.org/10.1038/nm.2807
53. Braithwaite AT, Marriott HM, Lawrie A. Divergent roles for TRAIL in lung diseases. *Front Med (Lausanne)*. 2018;5:212. https://doi.org/10.3389/fmed.2018.00212
54. Haw TJ, Starkey MR, Nair PM, et al. A pathogenic role for tumor necrosis factor-related apoptosis-inducing ligand in chronic obstructive pulmonary disease. *Mucosal Immunol*. 2016;9:859–872. https://doi.org/10.1038/mi.2015.111
55. Morissette MC, Parent J, Milot J. The emphysematous lung is abnormally sensitive to TRAIL-mediated apoptosis. *Respir Res*. 2011;12:105. https://doi.org/10.1186/1465-9921-12-105
56. Wu Y, Shen Y, Zhang J, et al. Increased serum TRAIL and DR5 levels correlated with lung function and inflammation in stable COPD patients. *Int J Chron Obstruct Pulmon Dis*. 2015;10:2405–2412. https://doi.org/10.2147/COPD.S92260
57. Abedini A, Zhu YO, Chatterjee S, et al. Urinary single-cell profiling captures the cellular diversity of the kidney. *J Am Soc Nephrol*. 2021;32:614–627. https://doi.org/10.1681/ASN.2020050757